Endogenous lipoid pneumonia associated with pulmonary neoplasia in three dogs

Endogenous lipoid pneumonia associated with pulmonary neoplasia in three dogs

Journal:	*Journal of Small Animal Practice*
Manuscript ID	JSAP-2018-0179.R1
Manuscript Type:	Case Report
Keywords:	Oncology, Canine, Pneumonia, Lipid, Neoplasia

Abstract

Endogenous lipoid pneumonia is a poorly characterized condition in veterinary medicine and there are very few reports describing this pathology, particularly in canine patients. However, it is a well-recognized pathology associated to lung neoplasia in humans. This case series describes three unique cases of endogenous lipoid pneumonia associated to lung neoplasia. The clinical, imaging, cytological findings and the outcome are described in dogs for the first time. Clinical presentation and imaging lesions can appear non-specific, and may be obscured by the presence of the neoplastic infiltrate. In order to diagnose this condition, cytology or histopathology is required. Awareness of the existence of endogenous lipoid pneumonia in dogs with pulmonary neoplasia can be crucial. It could have an impact in the staging and monitoring of these patients, in terms of their clinical signs and quality of life, alongside guiding the appropriate use of antimicrobials.

Introduction

Lipoid pneumonia is an uncommon condition characterized by the presence of intra-alveolar lipid and lipid-laden macrophages in the alveoli. The term lipoid pneumonia is more widely used in the human literature, whereas lipid pneumonia has been utilised in the veterinary field. It has been previously reported under other different names such as paraffinoma, cholesterol pneumonia and lipid granulomatosis (Hadda & Khilnani 2010). This condition is classified as being exogenous or endogenous, depending on the lipid source. Exogenous lipoid pneumonia is caused by a chronic foreign body reaction to fatty substances in the alveoli, typically after

inhalation or aspiration of laxative mineral oils, and has been widely described in human and veterinary medicine (Hadda &Khilnani 2010, Carminato *et al.* 2011).

Endogenous lipoid pneumonia (EnLP) has a more complex pathophysiology. It is thought to be caused by pneumocyte injury, leading to the alveolar lipid deposition. The causes proposed in the human literature include retained epithelial secretions, cell breakdown, vessel leakage, prolonged hypoxia, altered local oxygen and carbon dioxide tension, as well as dissemination of neoplastic cell breakdown products (Tamura *et al.* 1998). This condition is known to be associated with pulmonary neoplasia in human medicine (Tamura *et al.* 1998, Hadda &Khilnani 2010). Few reports in feline patients describe this condition together with pulmonary neoplasia (Jerram *et al.* 1998, Jones *et al.* 2000, Himsworth *et al.* 2008). To the authors' knowledge, EnLP secondary to lung tumours has not been reported in the veterinary literature.

This report characterizes the clinical findings, imaging features, cytological characteristics and outcome in three dogs diagnosed with EnLP in patients with pulmonary neoplasia.

Case histories

Case 1

A 12-year-old neutered female English springer spaniel, presented to a referral centre after an acute onset of lethargy and a non-productive cough.

Three months earlier, the dog had undergone a left caudal lung lobectomy following the discovery of a 2.5cm mass in thoracic radiographs. This lesion had been an incidental finding following the investigation of an acute hepatopathy. A moderately differentiated, completely excised pulmonary carcinoma was diagnosed on histopathology, WHO staging T1N0M0 (Owen

1980). Following the surgery, repeated imaging was performed by means of computed tomography (CT) to obtain a baseline prior to starting chemotherapy. At this time there was no evidence of recurrence or lymphadenopathy. The protocol consisted of vinorelbine 15mg/m^2, IV, q7 days for the first 4 weeks; after which there was still no radiographic evidence of tumour relapse or lymphadenopathy. Thereafter, the dog received the same dosage every 14 days. The dog received a total of six doses prior to representation.

On presentation, the dog was tachypnoeic with a respiratory rate of 60 breaths per minute and mild expiratory effort. Increased generalized bronchovesicular sounds and wheezes were noted on chest auscultation. The rectal temperature was 39.4°C. Diagnostic investigations included haematology, serum biochemistry and urinalysis, which were all unremarkable. Thoracic CT (Figure 1) revealed marked thickening of the bronchial walls (up to 6mm). This was associated with a patchy interstitial pattern in the surrounding lung parenchyma at the level of the cranial left lung lobe. The tracheobronchial lymph nodes and a left cranial mediastinal lymph node were enlarged. Generalized bullae were noticed as well.

Bronchoscopy was performed revealing thickened and narrow airways generally. Targeted bronchoalveolar lavages (BAL) of the right caudal and left cranial lung lobes were obtained. The cytological specimens were evaluated by a board-certified clinical pathologist. Cytologically, neutrophils predominated with a marked mucus background. High numbers of macrophages were also noted, alongside occasional Curshmann's spirals. This was suggestive of inflammation and chronic small airway disease. A few atypical epithelial cells were seen in the BAL sample, exfoliating in small groups. They had ahigh nucleus-to-cytoplasm ratio with a scant, deeply basophilic cytoplasm and often displayed two nucleoli. Anisocytosis and anisokaryosis were present in a moderate number of cells. These cells were suspicious for epithelial neoplasia.

Trans-thoracic ultrasound-guided fine-needle aspirates (FNA) of the left cranial lung lobe were obtained to confirm the diagnosis. Macroscopically, these had the appearance of lipid droplets (Figure 2A). Cytological evaluation revealed a background of lipid droplets. A population of round to polygonal cells exfoliating in cohesive clusters, of 20 to 40 µm in diameter was seen. They had a high nucleus-to-cytoplasm ratio, with scant deeply basophilic cytoplasm, and a centrally located round to bean-shaped nucleus with finely clumped chromatin and 1 to 2 prominent nucleoli. Bi-nucleation and nuclear moulding were seen and anisocytosis and anisokaryosis were marked. Several macrophages with numerous, clear vacuoles, and many neutrophils were also present (Figure 2B). Oil Red O stain revealed the vacuoles to be lipid accumulation, both free in the background and within the macrophages (Figure 2C). This was consistent with a carcinoma recurrence and secondary EnLP. Bacterial culture of the BAL fluid revealed a light, mixed bacterial growth suspected to be due to pharyngeal contamination. Based on the evidence of tumour recurrence, the chemotherapy protocol was changed to carboplatin (300mg/m^2 IV, q21 days), and prednisolone (1mg/kg PO q24h) was started in an attempt to address the lipoid pneumonia. The dog received two chemotherapy doses of this course in total. There was an initial improvement of the respiratory signs and general demeanour for the first month. However, thoracic radiographs were then repeated, showing a mild worsening of lung opacity in the region left caudal lung lobe consistent with tumour progression and/ or deterioration of the pneumonia. Three months after the diagnosis of EnLP was made, the patient acutely developed respiratory distress. Given the poor quality of life, guarded prognosis and limited evidence supporting other treatment options, the dog was humanely euthanized.

Case 2

As ix-year-old, neutered female, Labrador retriever was presented with a previous history of a squamous cell carcinoma(SCC) affecting digit five of the left forelimb a year prior to presentation. This had been completely excised by means of toe amputation and staged T1N0M0 at the time of the surgery. No follow up imaging was performed after this. More recently, the dog had developed a chronic, non-productive cough for the past three months. Thoracic radiographs obtained by the referring veterinary surgeons had identified a 4 cm soft tissue mass in the right middle lung lobe. Additionally, a new skin nodule was noted in the digit 3 of the right hind limb. This was completely excised by toe amputation and diagnosed as a novel SCC. The dog was then referred for further management for suspected metastatic SCC.

General physical examination was unremarkable; there was no evidence of recurrence at the previous surgical sites. Initial investigations included haematology and serum biochemistry, which were within normal limits. Thoracic CT identified multiple lung lesions in the right middle, right caudal, accessory and left cranial lung lobes. A 5.5 cm gas-filled mass was present in the right middle lung lobe (Figure 3A). It had an irregular, thick and mildly contrast-enhancing rim and was filled with hypoattenuating, non-contrast enhancing material (mean of 40 Hounsfield Units, HU). This mass was compressing the local airway, leading to collapse of the right middle bronchus and ventrally displacing the right cranial bronchus. Two other ventral soft tissue nodules could be seen: one in the right caudal lobe, measuring 6mm, and another one within in the accessory lobe, measuring 1cm. The cranial portion of the left cranial lobe was consolidated ventrally extending to a ground-glass opacity dorsally with its caudal portion becoming entirely consolidated. This area of the lung was heterogeneously contrast enhancing, creating a lobar sign. At this level, there was a 3cm diameter, non-contrast-enhancing, fluid dense mass (mean 25 HU) with an irregular, mildly contrast-enhancing rim. The

tracheobronchial lymph nodes were enlarged and heterogeneously enhancing, measuring up to 2.5 cm.

Given these findings, SCC metastasis was suspected. The 3cm nodule present in the caudal part of the left cranial lung lobe was sampled by means of ultrasound guided FNA. Upon smearing, the aspirate resembled lipid droplets macroscopically. The cytological specimens were evaluated by a board-certified clinical pathologist. On cytological examination, there were lipid vacuoles and several aggregates of foamy macrophages. A population of round to polygonal epithelial cells exfoliating in cohesive clusters were also identified. These cells had a basophilic cytoplasm, a round to irregular nucleus with finely stippled chromatin and the nucleolus was occasionally evident. Anisocytosis and anisokaryosis were moderate, and rare bi-nucleation with mitotic figures were present (Figure 4). A cytological diagnosis of SCC metastasis with associated EnLP was reached. Chemotherapy was declined by the owners, and a palliative course of meloxicam (0.1mg/kg PO q24h) and codeine (0.5mg/kg PO q12h) was started. In addition to pain relief and anti-inflammatory effects, meloxicam aimed at targeting Cox2 receptors possibly over expressed in the carcinoma. The dog developed acute lethargy, anorexia with increased respiratory effort several days after diagnosis, and the owners opted for euthanasia.

Case 3

A ten-year-old, neutered male, Weimaraner presented to a referral centre with a two month, progressive history of productive coughing, dysphonia and exercise intolerance. Inspiratory dyspnoea and tachypnoea were reported precipitated by exercise. On physical examination there was an evident stridor on inspiration. This was also noticeable upon laryngeal auscultation,

without adventitious lung sounds. The rest of the clinical and neurological examination was unremarkable. Given a clinical suspicion of laryngeal paralysis, a laryngeal assessment under general anaesthesia was planned. Haematology and serum biochemistry were unremarkable. Paradoxical motion of the arytenoid cartilages was detected, consistent with bilateral laryngeal paralysis. A thoracic CT scan revealed a 4.8 cm poorly enhancing, soft tissue attenuating mass (mean 49 HU) with a small focal area of mineralisation at the level of the left cranial lung lobe (Figure 5). Within the periphery of the right middle lung lobe there was increased attenuation with small air bronchograms present, and loss of lung volume. Bullae were also identified throughout the pulmonary parenchyma. These findings were suspicious of pulmonary neoplasia. The appearance of the right middle lung lobe was attributed to atelectasis, although a pneumonic focus (e.g. aspiration pneumonia) was included as a possible differential diagnosis. An abdominal CT scan was also performed for staging purposes, and was unremarkable. An ultrasound guided FNA of the mass in the left cranial lung lobe was obtained.

The cytological specimens were evaluated by a board-certified clinical pathologist. Cytology revealed a proteinaceous background with several lipid vacuoles and necrotic debris with calcium crystals. A population of neoplastic epithelial cells exfoliating in clusters was observed alongside numerous degenerate neutrophils, eosinophils, and a few macrophages containing lipid vacuoles. Epithelial cells were small, round to polygonal, with a high nucleus-to-cytoplasm ratio, a round to oval nucleus with finely stippled chromatin, and basophilic cytoplasm. Anisocytosis and anisokaryosis were moderate, and a few bi-nucleated cells were seen (Figure 6).These findings were consistent with epithelial neoplasia with necrosis, mixed inflammation and secondary EnLP.

A surgical left arytenoid lateralization was performed. The dog recovered uneventfully and was discharged from the hospital 48 hours after the surgery. Lung lobectomy was declined by the owners. At last follow up, four months after the surgery, the patient was clinically well with no clinical signs apparent to the owners.

Discussion

Endogenous lipoid pneumonia has been reported in a number of species in veterinary literature. It has been previously associated to parasitic lung disease (Brown 1988), heartworm infection, plant material aspiration (Hamir *et al.* 1996) and has been classified as idiopathic in some cases (Hamir *et al.* 1996; Hamir *et al.* 1997; Bollo *et al.* 2012). In addition, it has been reported in relation to neoplastic causes (Perpiñán *et al.* 2010) as well as atherosclerosis and hepatopathies (Costa *et al.* 2013).

In small animal medicine, EnLP is rare but has been more commonly diagnosed in cats. It was documented to be associated to obstructive pulmonary disease in 42% of cases in a retrospective study of 24 feline post-mortem examinations (Jones *et al.* 2000). These included two cases of neoplasia, both a primary and a metastatic lung carcinoma, as well as inflammatory, infectious and thromboembolic pulmonary conditions. In feline patients, other single pathology based case reports have identified EnLP in association with neoplastic diseases (Jerram *et al.* 1998; Himsworth *et al.* 2008) and bromide treatment (Bertolani *et al.* 2012).

There are a small number of reports of EnLP in dogs and the presenting signs, imaging, clinicopathological features and outcome are not well described. The first case report in a dog was suspected to be secondary to food inhalation (Corcoran *et al.* 1992). Since then, it has been seldom described but has been identified in association with infectious conditions such as

Dirofilaria immitis (Raya *et al.* 2006) and *Mycobacterium fortuitum* (Leissinger *et al.* 2015), as well as laryngeal paralysis(Camus *et al.* 2013).

The existing literature suggests that its clinical presentation consists of unspecific respiratory signs such as cough or tachypnoea (Jones *et al.* 2000, Hadda and Khilnani 2010). In the cases described above, the clinical signs of the dogs were non-specific and varied widely from cough to respiratory distress, which could also be explained by the presence of pulmonary neoplasia, or by the laryngeal paralysis in case three.

Radiographically, EnLP is known to present as solid opacities with or without central obstructive lesions (Tamura *et al.* 1998). Computed tomography can provide more accurate information regarding lung lesions location, nature and extent (Otoni *et al.* 2010; Marolf *et al.* 2011; Armbrust *et al.* 2012).Based on its location, EnLP has been further classified in human patients as: type I, localized in the parenchyma distally to the airway obstruction; type II, consecutively spreading to the adjacent segment where its own airway was not affected; or type III, spreading to other isolated segments (Tamura *et al.* 1998). However, unlike exogenous lipoid pneumonia, lipid-containing opacities with low attenuation are not expected on imaging (Betancourt *et al.* 2010). Furthermore, CT images can also show areas of ground-glass opacity superimposed on interlobular septal thickening (also referred as “crazy-paving pattern”); which is a non-specific finding (Betancourt *et al.* 2010; Byerley *et al.* 2016).

In the present case series, the areas cytologically confirmed as being EnLP displayed a number of imaging features. These included a patchy interstitial pattern; anon-contrast-enhancing, fluid dense mass with an irregular rim surrounded by consolidated and heterogeneously contrast-enhancing parenchyma; and a poorly contrast-enhancing, soft tissue attenuating mass.

Unfortunately, given the low number of cases, it is difficult to define the consistent imaging

features of this type of pneumonia in dogs. Given the variability already described in the literature and the concurrent presence of neoplastic infiltrates, there are likely no pathognomonic imaging findings for EnLP.Interestingly, two of the cases were found to have generalised bullae identified concurrently (cases one and three). The association between bullae and lung neoplasia is already described in human literature, with it reported that there is a relatively higher risk of lung cancer development in the wall of bullous lung disease in people, especially large cell carcinoma and SCC (Kaneda *et al.* 2010; Kimura *et al.* 2017). Further investigation is required to evaluate a potential connection between these and EnLP in dogs.

Given this clinical and radiological variability, definitive diagnosis requires cytological examination (BAL or trans-thoracic lung FNA) or histopathology to demonstrate lipid-laden macrophages with intra-alveolar lipid deposition (Hadda and Khilnani 2010). Special stains such as Oil Red O are available to detect lipid. Importantly, air-dried cytology specimens are preferred rather than methanol-fixed slides or routinely processed histologic samples; as alcoholic fixatives remove the lipid content from the sample (Masserdotti *et al.* 2006).The location of the lesions in the lung parenchyma could be considered as a limiting factor for sampling; although previous reports have shown no relevant complications of FNA regardless of the lesion location in the thorax(Zekas *et al.* 2005).

The main limitation of this report is the lack of post-mortem examination or histopathological evaluation for these cases. The presence of further post-mortem findings as well as the extent and severity of the lung lesions might have helped elucidate the aetiopathogenesis, clinical relevance and extent of EnLPin this group of dogs. Importantly, a number of different causes of lung injury have been reported to cause EnLP including drugs, inflammatory, infectious and thromboembolic lung disease. However, the co-existence of a separate lung pathology being the

main cause of EnLP in these cases is considered unlikely. The possibility of EnLP being a common underdiagnosed feature in a number of pulmonary conditions including neoplasia exists; and further studies evaluating the cytology and histopathology are warranted in at risk patients to investigate the relevance of EnLP in canine lung disease.

The mainstay of therapy for EnLP remains treating the underlying cause. There are no current specific treatment recommendations for this condition. Glucocorticoids are mentioned as a promising option based on anecdotal reports in human literature (Hadda and Khilnani 2010; Lococo *et al.* 2012), but these are recommended only if there is evidence of ongoing severe inflammation and associated clinical signs. Cytological diagnosis of lung lesions in these patients (BAL or FNA) is not only useful to confirm neoplasia and EnLP, but can also rule out infectious diseases such as bacterial pneumonia and prevent the inappropriate use of antimicrobials.

Given the non-specific presentation and imaging features, this condition might be underdiagnosed in canine patients with pulmonary neoplasia. Human literature suggests EnLP is a common finding, and was identified retrospectively in 22% extirpated lung tumours in one study (Tamura *et al.* 1998). The characterization of this condition in dogs is important, as EnLP might obscure the true extent of the neoplasia, hampering their diagnsosis and monitoring. For instance, EnLP could be misdiagnosed as tumour growth or as new metastatic lesions. This emphasizes the importance of its correct diagnosis by means of cytological evaluation. Hence, its incorrect interpretation may have an impact on staging and therapeutic decision-making in canine oncology patients. However, more information regarding this condition in dogs is needed to clarify if indeed it has a clinical implication in these patients; and will allow researchers to elucidate therapeutic options.

In conclusion, EnLP is a well-described condition in the human literature and is commonly reported in association with lung tumours. This is described in detail for the first time in three canine patients. As clinical and imaging findings appear to be non-specific, intracellular and extracellular lipid on cytology or histology are required for the diagnosis to be made. A failure to consider and recognise EnLP in dogs with pulmonary neoplasia could have a negative impact on the staging and monitoring of pulmonary neoplasia. Further large scale studies are warranted to investigate the prevalence of EnLP in dogs with pulmonary neoplasia and to explore its possible impact on treatment and prognosis.

References

Armbrust, L.J., Biller, D.S., Bamford, A. *et al.*(2012) Comparison of three-view thoracic radiography and computed tomography for detection of pulmonary nodules in dogs with neoplasia. *Journal of the American Veterinary Medical Association* 240(9), 1088–1094.

Bertolani, C., Hernandez, J., Gomes, E., *et al.*(2012) Bromide-associated lower airway disease: a retrospective study of seven cats. *Journal of Feline Medicine and Surgery* 14(8), 591–597.

Betancourt, S.L., Martinez-Jimenez, S., Rossi, S.E., *et al.*(2010)Lipoid pneumonia: Spectrum of clinical and radiologic manifestations. *American Journal of Roentgenology* 194(1), 103–109.

Bollo, E., Scaglione, F.E. & Chiappino, L.,*et al.*(2012)Endogenous lipid (cholesterol) pneumonia in three captive Siberian tigers (*Panthera tigris altaica*). *Journal of Veterinary Diagnostic Investigation* 24(3), 618–620.

Brown, C.C.(1988) Endogenous lipid pneumonia in opossum from Louisiana. *Journal of Wildlife Diseases* 24(2), 214–219.

Byerley, J.S., Hernandez, M.L., Leigh, M.W.,*et al.*(2016)Clinical approach to endogenous lipoid pneumonia. *The Clinical Respiratory Journal* 10(2), 259–263.

Camus, M., Cazzini, P., Beck, J.,*et al.*(2013) What is your diagnosis? An endotracheal wash from a dyspneic 3-month-old female Labrador Retriever. *Veterinary Clinical Pathology* 42(4), 527–528.

Carminato, A., Vascellari, M., Zotti, A., *et al.* (2011). Imaging of exogenous lipoid pneumonia simulating lung malignancy in a dog. *Canadian Veterinary Journal* 52(3), 310–312.

Corcoran, B.M., Martin, M., Darke, P.G.G.,*et al.*(1992)Lipoid pneumonia in a rough collie dog. *Journal of Small Animal Practice* 33(11), 544–548.

Costa, T., Grífols, J. & Perpiñán, D. (2013) Endogenous lipid pneumonia in an african grey parrot (*Psittacus erithacus erithacus*). *Journal of Comparative Pathology* 149(2-3), 381–384.

Hadda, V. & Khilnani, G.C.(2010) Lipoid pneumonia: an overview. *Expert Review of Respiratory Medicine* 4(6), 799–807.

Hamir, A.N., Andreasen, C.B. & Pearson, E.G.(1997) Endogenous lipid pneumonia (alveolar histiocytosis) and hydrocephalus in an adult llama (*Llama glama*). *The Veterinary record* 141(18), 474–475.

Hamir, A.N., Rupprecht, C.E. & Hanlon, C.A.(1996) Endogenous lipid pneumonia (multifocal alveolar histiocytosis) in raccoons (*Procyon lotor*). *Journal of Veterinary Diagnostic*

Investigation 8, 267–269.

Himsworth, C.G., Malek, S., Saville, K.,*et al.*(2008) Pathologists' Corner. Endogenous lipid pneumonia and what lies beneath. *Canadian Veterinary Journal* 49, 813–815.

Jerram, R.M., Guyer, C.L., Braniecki, A.,*et al.*(1998)Endogenous lipid (cholesterol) pneumonia associated with bronchogenic carcinoma in a cat. *Journal of the American Animal Hospital Association* 34(4), 275–80.

Jones, D.J., Norris, C.R.,Samii, V.F.,*et al.*(2000)Endogenous lipid pneumonia in cats: 24 cases (1985-1998). *Journal of the American Veterinary Medical Association* 216(9), 1437–1440.

Kaneda, M.,Tarukawa, T., Watanabe, F.,*et al.*(2010) Clinical features of primary lung cancer adjoining pulmonary bulla. *Interactive cardiovascular and thoracic surgery*10(6), 940–4.

Kimura, H., Saji, H., Miyazawa, T., *et al.*(2017) Worse survival after curative resection in patients with pathological stage I non-small cell lung cancer adjoining pulmonary cavity formation. *Journal of Thoracic Disease* 9(9), 3038–3044.

Leissinger, M.K., Garber, N., Fowlkes, N., *et al.*(2015) Mycobacterium fortuitum lipoid pneumonia in a dog. *Veterinary pathology* 52(2), 356–9.

Lococo, F., Cesario, V., Porziella, V., *et al.*(2012) Idiopathic lipoid pneumonia successfully treated with prednisolone. *Heart and Lung: Journal of Acute and Critical Care* 41(2), 184–187.

Marolf, A.J., Gibbons, B.K., Podell, R.D.P,*et al.* (2011) Computed tomographic appearance of primary lung tumors in dogs. *Veterinary Radiology and Ultrasound* 52(2), 168–172.

Masserdotti, C., Bonfanti, U., De Lorenzi, D.,*et al.*(2006) Use of Oil Red O stain in the cytologic

311 diagnosis of canine liposarcoma. *Veterinary Clinical Pathology* 35(1), 37–41.

312 Otoni, C.C., Rahal, S., Vulcano, L., *et al.*(2010)Survey radiography and computerized
313 tomography imaging of the thorax in female dogs with mammary tumors. *Acta Veterinaria*
314 *Scandinavica* 52(1), 6–9.

315 Owen, L., (1980) TNM Classification of tumours in domestic animals. *World Health*
316 *Organisation*, 1–52.

317 Perpiñán, D., Steffen, D. & Napier, J.E.(2010) Pulmonary adenocarcinoma and endogenous lipid
318 pneumonia in a common genet (*Genetta genetta*). *Journal of zoo and wildlife medicine:*
319 *official publication of the American Association of Zoo Veterinarians* 41(4), 710–712.

320 Raya, A.I., Fernandez-de Marco, M., Nunez, J.C.A., *et al.*(2006) Endogenous Lipid Pneumonia
321 in a Dog. *Journal of Comparative Pathology* 135(2-3), 153–155.

322 Tamura, A., Hebisawa, A., Fukushima, K., *et al.*(1998) Lipoid Pneumonia in Lung Cancer:
323 Radiographic and Pathological Features. *Japanese Journal of Clinical Oncology* 28(8),
324 492–496.

325 Zekas, L.J., Crawford, J.T. & O'Brien, R.T.(2005) Computed tomography-guided fine-needle
326 aspirate and tissue-core biopsy of intrathoracic lesions in thirty dogs and cats. *Veterinary*
327 *Radiology and Ultrasound* 46(3), 200–204.

328

329 **Conflict of interest**

330 None of the authors of this article have a financial or personal relationship with any individuals
331 or organizations that could influence or bias the content of this study.

332

333

334

335

336

337

338

339

340

341

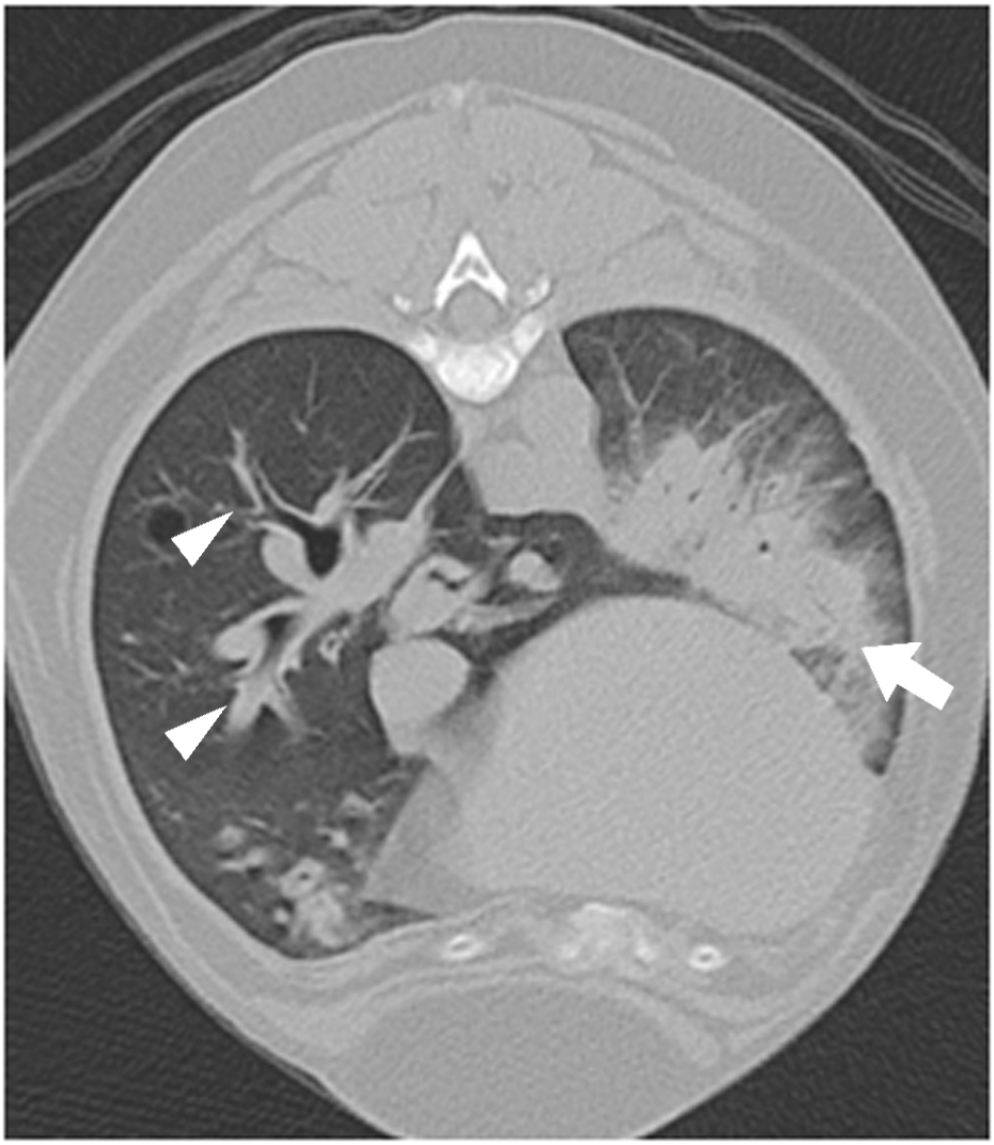

Figure 1:Transverse thoracic computed tomographic image at the level of T6 of a 12-year-old neutered female English springer spaniel. Moderate generalized bronchial wall thickening (arrowheads) and a patchy interstitial lung pattern (arrow) are visible. (Lung window). T: thoracic vertebra.

79x91mm (300 x 300 DPI)

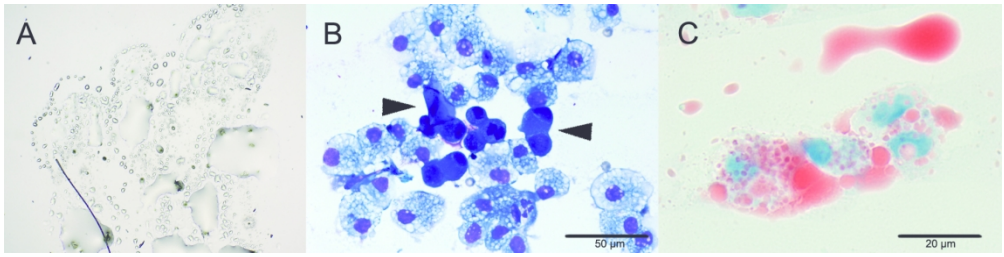

Figure 2: Macroscopic and microscopic findings from fine-needle aspirate in case 1. Macroscopically, the sample resembled lipid droplets (Figure A). Epithelial neoplastic cells (arrowheads), with a background of vacuolated macrophages and neutrophils were present (Figure B). Modified Giemsa, 40x, bar 50um. Oil Red O stain confirmed the vacuoles to be lipid accumulation (Figure C). Oil Red O, 100x, bar 20um.

163x40mm (300 x 300 DPI)

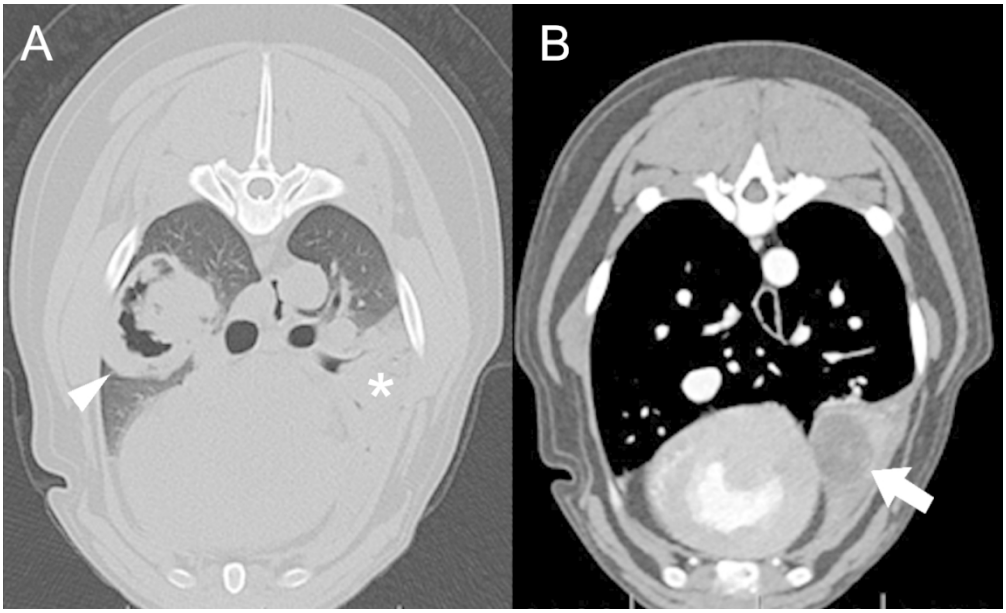

Figure 3: Transverse thoracic computed tomographic images at the level of T5 (A) and T7 (B) of a 6-year-old neutered female Labrador retriever. Note the large pulmonary gas-filled mass (A) (arrowhead, lung window) and the left cranial lung lobe consolidation (asterisk). Note the fluid dense mass located on the caudal aspect of the cranial lung lobe (B) (white arrow, soft tissue window post contrast).T: thoracic vertebra.

116x70mm (300 x 300 DPI)

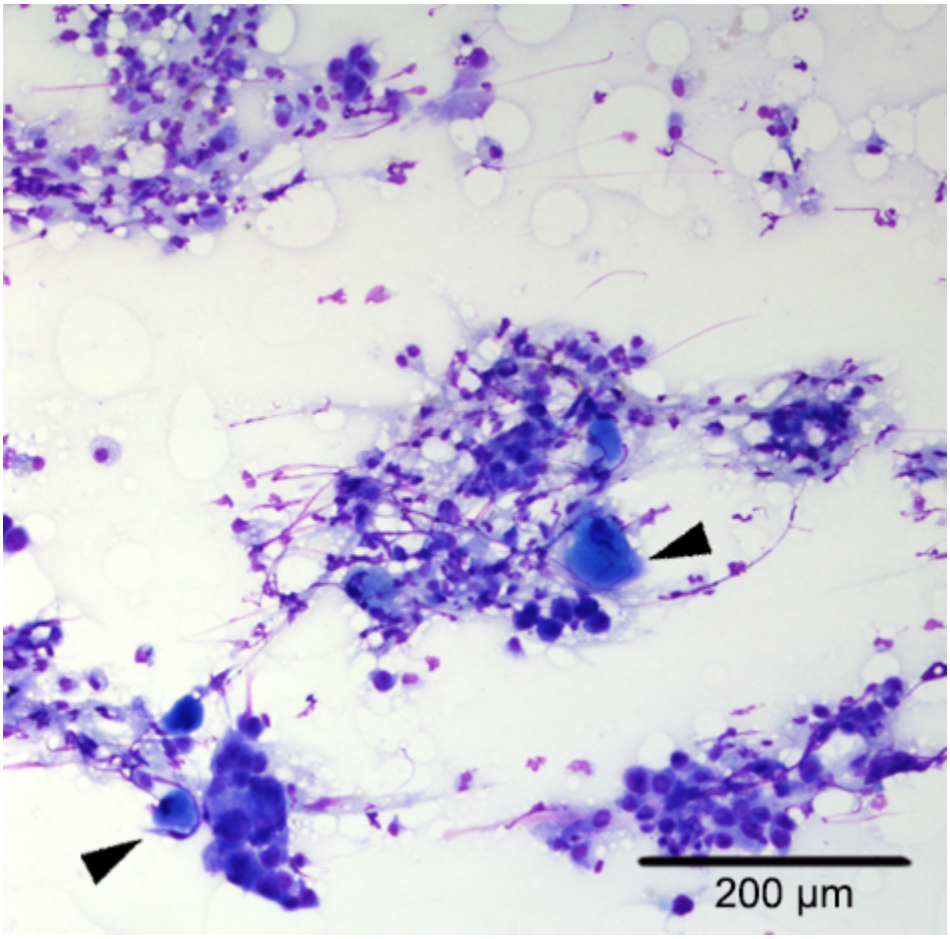

Figure 4: Microscopic findings from fine-needle aspirate in case 2. Notice the presence of lipid droplets and inflammatory cells (neutrophils and lipid-laden macrophages) in the background, and a population of epithelial neoplastic cells with some squamous cell differentiation (arrowheads). Modified Giemsa, 10x, bar 200um.

39x39mm (300 x 300 DPI)

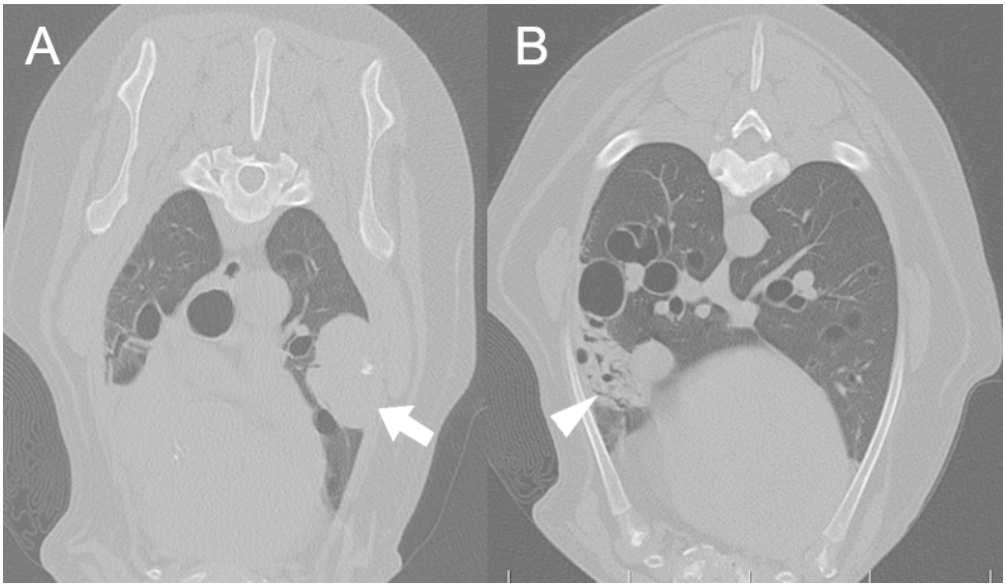

Figure 5: Transverse thoracic computed tomographic images at the level of T4 (A) and T7 (B) of a 10-year-old neutered male Weinmaraner. Note the soft tissue attenuating mass (A) (white arrow, lung window). Note an area of increased attenuation and loss of lung volume (B) (arrowhead, lung window). T: Thoracic vertebra.

67x38mm (300 x 300 DPI)

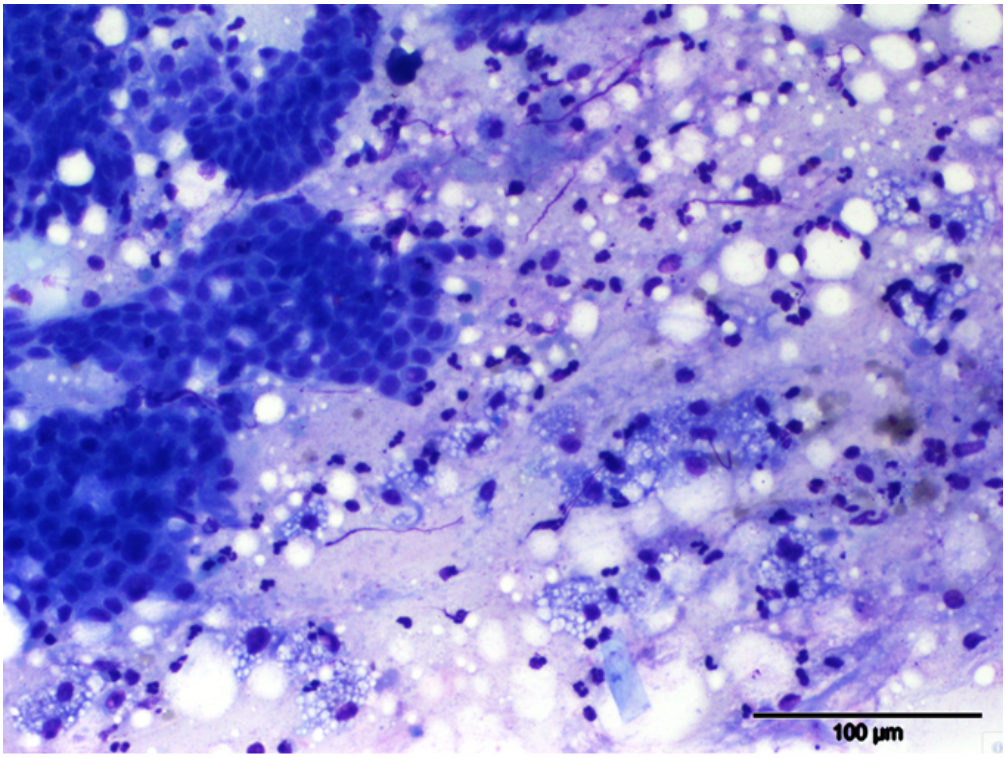

Figure 6: Microscopic findings from fine-needle aspirate in case 3. Cytological evaluation revealed a background of lipid droplets and a population of epithelial neoplastic cells was seen (arrows). Several macrophages with numerous, clear, well-defined vacuoles (arrowheads) and many neutrophils were also present (Modified Giemsa, 10x, bar 100um).

239x179mm (72 x 72 DPI)